AUTONOMOUS CONSTRAINED CONTROL FOR ARBITRARY CONFIGURATIONS OF GIMBALING THRUSTERS IN SE(3)

Matthew M. Wittal[*], Morad Nazari[†]

In order to develop robust autonomy in spacecraft, it is desirable to develop methods for controlling a spacecraft in various configurations with any combination of thrusters of various types and both for static RCS thrusters and gimbaling thrusters. In the case of a stuck thruster imposing unplanned and undesired motion both translational and rotational or in the case of a malfunctioning thruster, it is desirable for that spacecraft to have the ability to identify and overcome that problem without human intervention. To that end, a spacecraft must be able to rapidly and autonomously reconfigure thruster firing histories and update guidance protocols. In this paper, a method for a spacecraft to autonomously select thrusters of any configuration is presented. The residual motion imposed by off-nominal or not-fully-controllable thruster configurations is identified by the spacecraft and solved for, both for static reaction control systems and gimbaling engines.
Keywords:SE(3), GN&C, autonomy

INTRODUCTION

Any permanent human settlement requires a degree of logistics in order to sustain itself. Historically, logistics took the form of sending lumber down rivers, using horse and carriage, and eventually progressed to complex supply chains involving several mediums for the transportation of goods and people. The Artemis program's current goal of establishing the first permanently manned colony on the surface of the Moon will necessitate the use of logistics vehicles to deliver supplies to and from the Lunar surface, and necessitates the creation of robust autonomous methodologies to ensure the reliable performance of these spacecraft. Furthermore, the inevitable successor to the Artemis program that seeks to put humans on Mars will further demand the development of multi-use spacecraft capable of transporting a wide range of cargo. This suggests that a notional control scheme most be robust to a wide range of scenarios. In this work, the cases of malfunctioning thrusters is explored, and it is demonstrated that using the algorithm described herein that a spacecraft can overcome unplanned configurations of thrusters. The spacecraft configuration is defined within the $\mathsf{SE}(3)$ framework. This allows a spacecraft to consider both the translational and rotational component of it's thruster configuration simultaneously, and aids in generating precise guidance protocols even in the presence of sub-optimal and off-nominal thruster configurations.

SPECIAL EUCLIDEAN GROUP $\mathsf{SE}(3)$

The pose of a rigid body is expressed by a combination of 6 degrees of freedom, 3 rotational and 3 translational. This pose may be modeled in $\mathsf{SE}(3)$ as

$$g = \begin{bmatrix} R & r \\ 0_{1\times 3} & 1 \end{bmatrix} \in \mathsf{SE}(3) \tag{1}$$

[*]Automation and Robotics Systems Engineer, Granular Mechancis and Regolith Operations Laboratory, NASA Kennedy Space Center, FL 32899, and Ph.D. Candidate, Embry-Riddle Aeronautical University, 1 Aerospace Blvd., Daytona Beach, FL 32114
[†]Assistant Professor, Aerospace Engineering, Embry-Riddle Aeronautical University, Daytona Beach, FL 32114

where $R \in \mathsf{SO}(3)$ is the attitude expressed as a rotation matrix and r is the position vector in the inertial frame. Note that the rotation matrix rotates from a rigid body frame $\mathcal{B}$ to some inertial frame $\mathcal{N}$. The rigid body's velocity can be defined using an augmented velocity vector $\mathbb{V}$ as

$$\mathbb{V} = \begin{bmatrix} \omega \\ v \end{bmatrix} \in \mathbb{R}^6 \tag{2}$$

such that $\omega \in \mathbb{R}^3$ is the angular velocity in the body frame $\mathcal{B}$ and $v \in \mathbb{R}^3$ is the translational velocity relative to the inertial frame and expressed in the body frame. For the purposes of developing a relative motion or tracking controller, consider the formulation for relative poses on $\mathsf{SE}(3)$, expressed as $g_{i/j} = g_j^{-1} g_i$, and take the linear adjoint operator of this relative configuration to yield

$$\mathrm{Ad}_{g_{\mathcal{M}/\mathcal{B}}} = \begin{bmatrix} R_{\mathcal{M}/\mathcal{B}} & 0 \\ r^{\times}_{\mathcal{M}/\mathcal{B}} R_{\mathcal{M}/\mathcal{B}} & R_{\mathcal{M}/\mathcal{B}} \end{bmatrix} \tag{3}$$

The transpose of the adjoint operator is defined as

$$\mathrm{Ad}^T_{g_{\mathcal{M}/\mathcal{B}}} = \begin{bmatrix} R^T_{\mathcal{M}/\mathcal{B}} & -R^T_{\mathcal{M}/\mathcal{B}} r^{\times}_{\mathcal{M}/\mathcal{B}} \\ 0 & R^T_{\mathcal{M}/\mathcal{B}} \end{bmatrix} \tag{4}$$

And finally,

$$\mathrm{Ad}^T_{g^{-1}_{\mathcal{M}/\mathcal{B}}} = \begin{bmatrix} R_{\mathcal{M}/\mathcal{B}} & R_{\mathcal{M}/\mathcal{B}} \left(R^T_{\mathcal{M}/\mathcal{B}} r_{\mathcal{M}/\mathcal{B}} \right)^{\times} \\ 0 & R_{\mathcal{M}/\mathcal{B}} \end{bmatrix} \tag{5}$$

Now the relative pose between the estimated state and the desired state may be expressed as

$$\begin{aligned} \epsilon_g &= g_d^{-1} \hat{g} = \begin{bmatrix} \hat{R}_d & \epsilon_r \\ 0 & 1 \end{bmatrix} = \begin{bmatrix} R_d^T \hat{R} & R_d^T (\hat{r} - r_d) \\ 0 & 1 \end{bmatrix} \\ \epsilon_{\mathbb{V}} &= \hat{\mathbb{V}} - \mathrm{Ad}_{\hat{\mathbb{V}}} \mathbb{V}_d \end{aligned} \tag{6}$$

where the subscript d denotes the desired or modeled state or parameter. The relative dynamics of a rigid body with a changing center of mass and moments of inertia in $\mathsf{SE}(3)$ are represented in the dynamic model as

$$\dot{\epsilon}_g = \epsilon_g \epsilon_{\mathbb{V}}^{\vee} \tag{7a}$$

$$\dot{\epsilon}_{\mathbb{V}} = \mathbb{I}^{-1} \left(\mathrm{ad}^*_{\epsilon_{\mathbb{V}}} \mathbb{I} \epsilon_{\mathbb{V}} + \tau + u \right) \tag{7b}$$

where

$$\mathbb{I} = \begin{bmatrix} J & 0_{3\times3} \\ 0_{3\times3} & mI_3 \end{bmatrix} \in \mathbb{R}^{6\times6}, \tag{8}$$

Here, $J \in \mathbb{R}^{3\times3}$ is the moment of inertia about the center of mass, and $m \in \mathbb{R}$ is the mass of the body. It is assumed that $\mathbb{I}$ is time-varying, and its rate of change with respect to time is

$$\dot{\mathbb{I}} = \begin{bmatrix} \dot{J} & 0_{3\times3} \\ 0_{3\times3} & \dot{m}I_3 \end{bmatrix} \in \mathbb{R}^{6\times6} \tag{9}$$

The co-adjoint operator is defined as

$$\mathrm{ad}^*_{\mathbb{V}} = \mathrm{ad}^T_{\mathbb{V}} = \begin{bmatrix} -\omega^{\times} & -v^{\times} \\ 0_{3\times3} & -\omega^{\times} \end{bmatrix} \in \mathbb{R}^{6\times6} \tag{10}$$

where the adjoint operator $\mathrm{ad}_{\mathbb{V}}$ is

$$\mathrm{ad}_{\mathbb{V}} = \begin{bmatrix} \omega^{\times} & 0_{3\times3} \\ v^{\times} & \omega^{\times} \end{bmatrix} \in \mathbb{R}^{6\times6} \tag{11}$$

In Eq. (7), $\tau = [L^T, f^T]^T \in \mathbb{R}^6$ represents the impressed dynamics acting on the system, where $L \in \mathbb{R}^3$ represents all external torques and $f \in \mathbb{R}^3$ represents all external forces, both of which are expressed in the $\mathcal{B}$ frame. Furthermore, the augmented vector of control inputs is given by $u = \left[u_L^T, u_f^T \right]^T$ where $u_L \in \mathbb{R}^3$ represents control torques and $u_f \in \mathbb{R}^3$ represents control forces.

TUG-CARGO SPACECRAFT CONFIGURATION ON $\mathsf{SE}(3)$

Consider a thruster whose pose is defined as

$$g_n = \begin{bmatrix} R^{\mathfrak{B}}_{\mathfrak{M}} & r^{\mathfrak{M}} \\ 0_{1\times 3} & 1 \end{bmatrix} \tag{12}$$

where $R^{\mathfrak{B}}_{\mathfrak{M}}$ is the attitude of the thruster in body frame $\mathfrak{B}$, and $r^{\mathfrak{M}}$ is the position of the body with respect to the thruster.

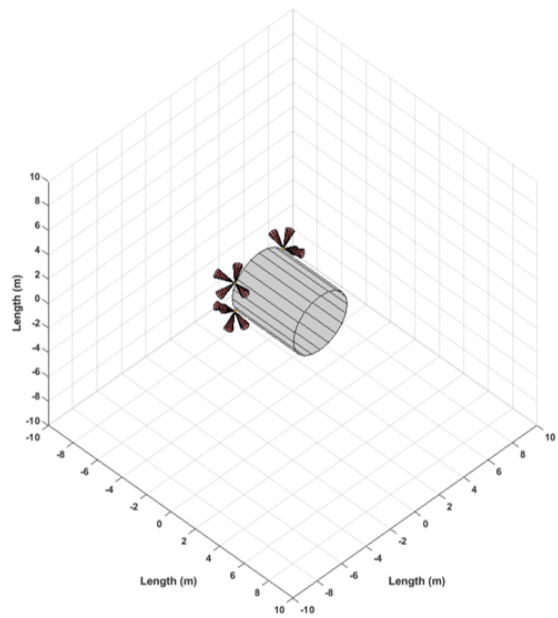

Figure 1: The configuration of a spacecraft with all thrusters located on one side, with a center of mass that lies well outside of the geometric center of the thrusters.

AUTONOMOUS GUIDANCE AND CONTROL

Ongoing work seeks to improve the contributions in [1] by developing a higher fidelity control methodology composed of two parts: distributed constrained control, and saturation limits for both the thrust gimbaling and gimbaling rate. Define an actuator $g_{\mathcal{M}} \in \mathsf{SE}(3)$ where $\mathcal{M}$ denotes the frame of the actuator with respect to the rigid body. For a distributed control scheme within the $\mathsf{SE}(3)$ framework, consider an arbitrary control input in the body frame $u \in \mathbb{R}^6$. It is desired to determine how this control input is distributed about various actuators and how it determines the gimbling of those actuators. Regarding the first item and for simplicity, a homogeneous distribution of total thrust capacity may be assumed such that $u = \sum_{n=1}^{N} u_n$ where u_n is the control input on the nth actuator and N is the total number of actuators. It can be seen that $\text{Ad}_{g_{\mathcal{M}}^{-1}} u_n$ will fully compute the torques and forces acting on the rigid body from the control inputs centered at the nth actuator in N. As a result, the final control acceleration acting on the rigid body from the nth actuator can be given as

$$a_u = \mathbb{I}^{-1} \text{Ad}_{g_{\mathcal{M}}^{-1}} u \tag{13}$$

This expression is convenient because the control inputs in the $\mathcal{M}$ frame should be known based on actuator specifications and the actuator's configuration relative to the rigid body should also be known based on the rigid body's design parameters. However, for gimbaling actuator with actuation limits both the gimbal limits and the gimbal rate limits of that actuator must be considered. Since the actuators are not static, one must consider the desired control input $u_{d,n} = [T_{d,n}, f_{d,n}]^T$ as distinct from the true control output

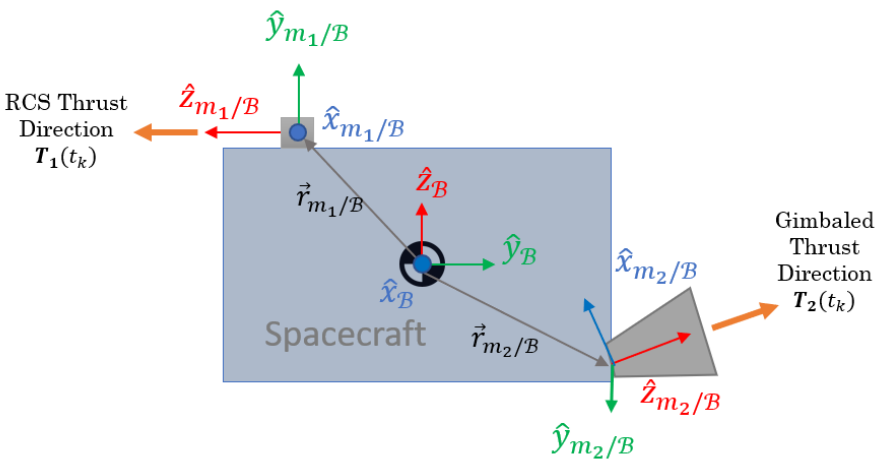

Figure 2: The configuration of a spacecraft with n number of thrusters of various types.

$u_{act,n} = [T_{act,n}, f_{act,n}]^T$ to determine the new orientation for the actuators. To do this, the individual contributions each thruster has to the translational and rotational motion of the central body are assessed by

$$x_n = -\left(R_{\mathcal{M}/\mathcal{B},n}\hat{e}_3\right) \cdot u_f$$
$$\forall\, x_n \leq 0, \tag{14}$$
$$f_n = ||-\left(R_{\mathcal{M}/\mathcal{B}}\hat{e}_3 \cdot u_f\right) u_{f,d}|| \tag{15}$$
$$\text{otherwise}, f_n = 0 \tag{16}$$

such that $\hat{e}_{3,\mathcal{M}} = [0,0,1]^T_{\mathcal{M}}$ is the 3rd basis vector of the motor frame. This function assigns a zero value to the torque if the desired translational motion is in the opposing direction and n is the number of actuators in the system of interest, as illustrated in Figure 2. Inversely, an attitude maneuver with excess torque components may induce undesirable translational components. A similar analysis may be performed in reverse, by summing the torques

$$x_n = \left(R_{\mathcal{M}/\mathcal{B},n} r_{\mathcal{M},n}\right)^{\times} R_{\mathcal{M}/\mathcal{B},n}\hat{e}_{3,\mathcal{M}} \cdot u_T$$
$$\forall\, x_n \leq 0, \tag{17}$$
$$T_n = ||-\left(\left(R_{\mathcal{M}/\mathcal{B},n} r_{\mathcal{M},n}\right)^{\times} R_{\mathcal{M}/\mathcal{B},n}\right) \cdot u_T)\, u_T|| \tag{18}$$
$$\text{otherwise}, T_n = 0 \tag{19}$$

The vectors produced by Eqs. 14 and 17 describe the required ratio of duty cycles required to compensate for a maneuver. It is of note that the T_n and f_n vectors are normalized because differences in the magnitude of thruster inputs in various directions may be overcome by implementing duty cycles. This assumption breaks down when there are discrepancies of an order of magnitude of more, in which case these components can be neglected using a duty cycle limit threshold β, which is specific to the system of interest. For example, in a notional system in which thursters are cycled at 1 Hz for a maximum on time of 1 second and a minimum on time of 0.1 seconds, β = 10. Next, the full control vector is assembled as

$$U = \begin{bmatrix} T_1, T_2, ..., T_n \\ f_1, f_2, ..., f_n \end{bmatrix} \in \mathbb{R}^{6\times n} \tag{20}$$

In order to implement these values into a system with discrete on-times, such as a Reaction Control System, our control matrix U may be discretized into fractional values that are rounded to the nearest appropriate decimal value (e.g., $\frac{1}{10}, \frac{2}{10}$... etc.) as determined by the system of interest and the maximum whole number

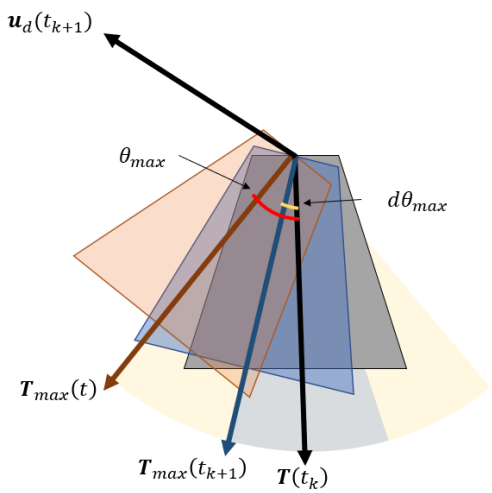

Figure 3: The configuration of a gimbaling rocket motor with the nomenclature that is used in this work.

value in U. Total adjusted control of the system may be expressed as $u_{act} = \sum_{n=1}^{N} u_{act,n} = \sum_{n=1}^{N} U_n$ where U_n is the nth column of U.

The methodology described so far is adequate for addressing infeasible control inputs for an arbitrary configuration of stationary reaction control system thrusters. Now but gimbal limits and gimbal rate limits must be considered for dynamic thruster configurations, such as rocket engines. First, to interpret the performance limitations of gimbaling thrusters, the new spacecraft actuator configuration may be treated as though a thruster exists at the extremes of the gimbal limits in either direction, as illustrated in Fig. 3.

A gimbaling thruster is usually incapable of actuating between the limits during a single given time step. This constraint is imposed by considering the difference between the current actuator configuration and the desired actuator configuration and applying an angular rate limitation in the rotational direction of the desired control configuration in the actuator frame. In Figure 3, the initial configuration of the rocket motor is given by $\mathbf{T}_k$, or the direction of thrust at time step k. The desired control input is given by $\mathbf{u}_d(t_{k+1})$. However, the maximum gimbal rate for a time step dk is given by the blue motor position $\mathbf{T}_{max}(t_{k+1})$, and the maximum angular displacement for that time step $d\theta_{max}$. Furthermore, the gimbal limits of the motor for any time is given by $\mathbf{T}_{max}(t)$ as well as the maximum angular displacement of the motor θ_{max}.

To impose these constraints, a gimbal rotation matrix using the thrust vector and desired control vector as basis functions to construct a rotation matrix is assembled. So long as the final angular displacement does not exceed θ_{max} and the difference between the current thrust vector and the desired thrust vector is greater than $d\theta_{max}$, the gimbal attitude $R_{m/\mathcal{B}}$ can be multiplied by a rotation matrix about the third axis $R_3(d\theta_{max})$ to generate our new motor configuration.

To impose these constraints, we compose a gimbal rotation matrix using the following basis function:

$$\begin{aligned} \hat{m}_2 &= \frac{\mathbf{T}(t_k)}{|\mathbf{T}(t_k)|} \\ \hat{m}_3 &= \frac{\mathbf{u}_d(t_{k+1})^{\times}\hat{m}_2}{|\mathbf{u}_d(t_{k+1})|} \\ \hat{m}_1 &= \hat{m}_2 \times \hat{m}_3 \\ R_{m/\mathcal{B}} &= [\hat{m}_1, \hat{m}_2, \hat{m}_3] \end{aligned} \tag{21}$$

So long as the final angular displacement does not exceed θ_{max} and the difference between the current

thrust vector and the desired thrust vector is greater than $d\theta_{max}$, we can multiply the gimbal attitude $R_{m/\mathcal{B}}$ by a rotation matrix about the third axis $R_3(d\theta_{max})$ to generate our new motor configuration.

SIMULATION

Two simulations are considered: the case of a tug-cargo spacecraft configurations with RCS thrusters and the case of a Falcon 9 rocket. in Fig. 4, the thruster firing history for a set of RCS thrusters on a tug-cargo configured spacecraft has been autonomously determined for 6 different scenarios, one corresponding to desired motion in each degree of freedom. In all cases, thruster firings were discritized into 1/16 second units, with a maximum duty cycle and on-time of 1 Hz.

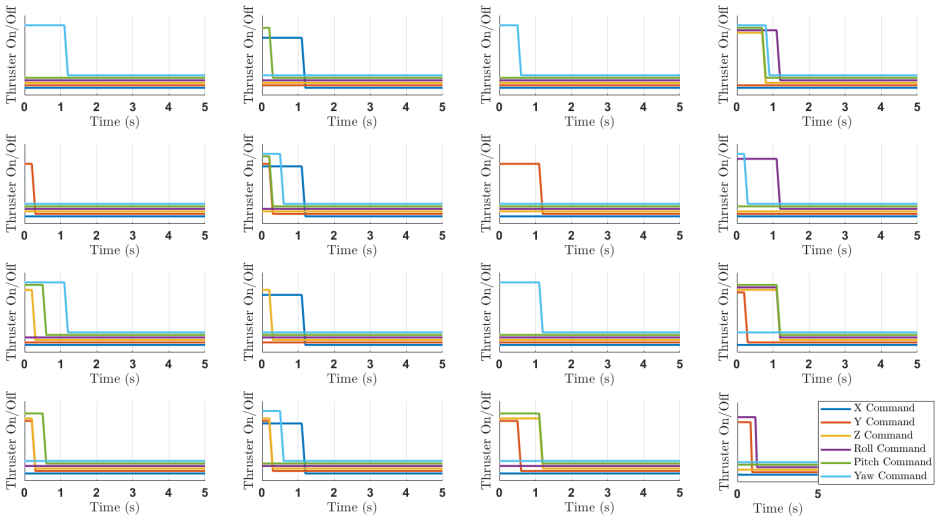

Figure 4: The autonomously generated thruster firing history for maneuvers about each principle axes in the translational and rotational directions.

The residual motion caused by these various commands is explored in Fig. 5, which illustrates the velocity during and after thruster firings. Some thruster firing commands are not perfectly controlled motion, i.e., scenarios in which there is residual motion about other axes than the one desired. When considering a tug-cargo configuration, it is not surprising that there is residual motion about the y- and z-axis especially, since only the x- and roll-axis are intuitively completely controllable.

Fig 6 shows the thrusters of a Falcon 9 gimbaling autonomously when given a pitch command. Each engine is capable of moving independently, and more complicated commands - both control and guidance - are being explored and will be featured in the final paper.

EXPECTED RESULTS

Based on the initial results presented above, the final paper will incorporate duty cycle considerations for RCS thrusters in combination with gimbal and gimbal rate limits to assemble a guidance algorithm that incorporates the constraints of the given control system. Off-nominal scenarios of known spacecraft configurations will be considered, both for stuck thrusters and failed thrusters. The spacecraft, given no prior knowledge of which thruster is malfunctioning, will identify the problem and overcome it by disabling the thruster in question.

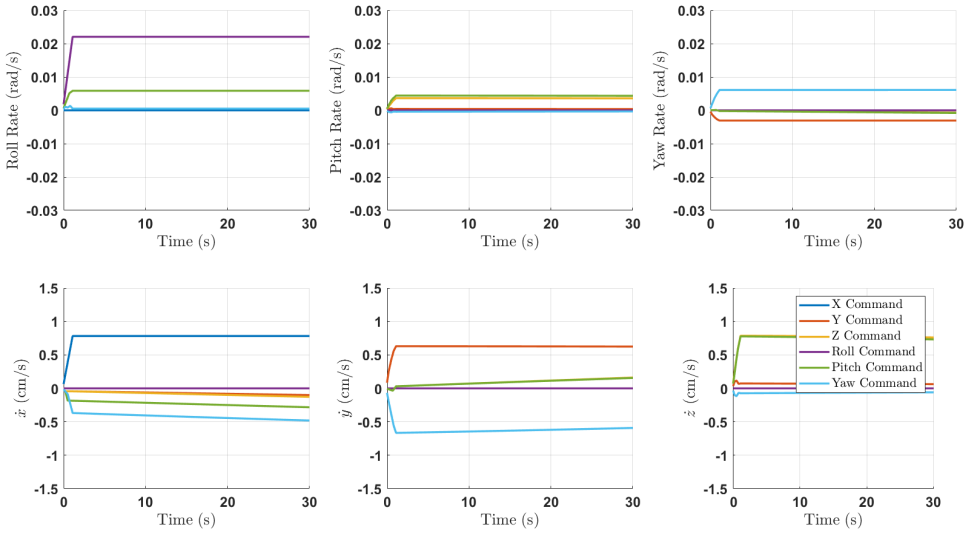

Figure 5: The resulting displacement and residual motion components for a spacecraft in a tug-cargo configuration.

REFERENCES

[1] M. M. Wittal, B. McCann, J. Benavides, and M. Nazari, "Ambiguity Remediation in Launch Vehicles with Parameter Uncertainties: A Comparison between Special Euclidean Group and Dual Quaternion," in *AIAA/AAS Astrodynamics Specialist Conference*, vol. 22-623, 2022.

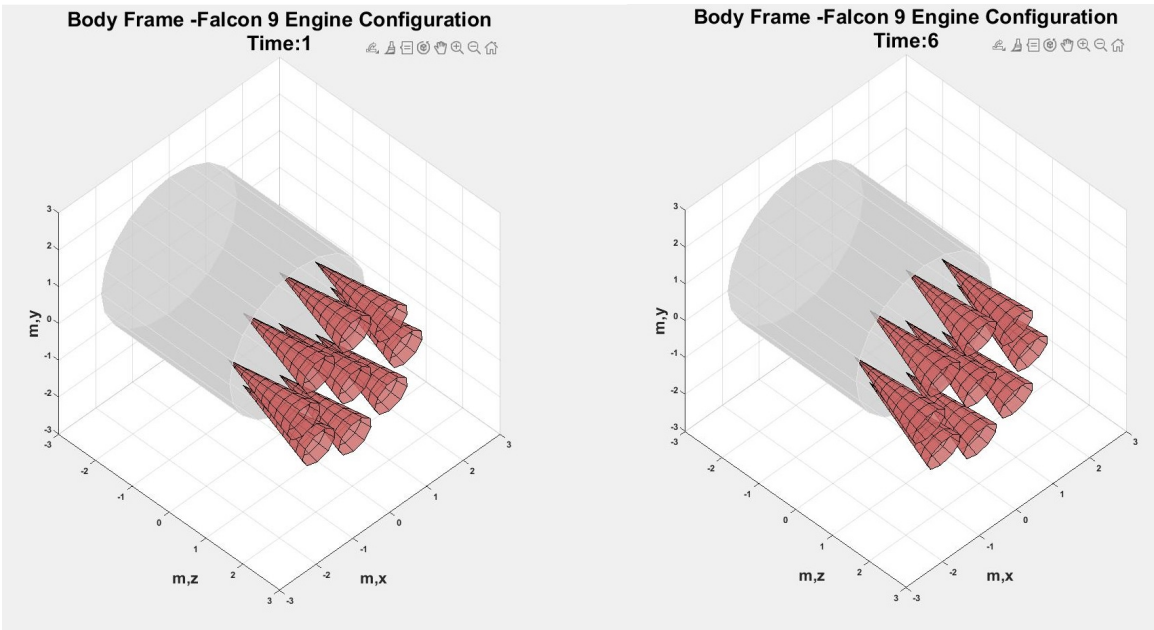

Figure 6: Autonomous gimbaling of a Falcon 9's thrusters that can recognize gimbal and gimbal rate limits for coupled motion.